

哈尔滨工程大学  
HARBIN ENGINEERING UNIVERSITY

# Single and Double Diffractive Production of Dilepton and Photon at Large Hadron Collider

Speaker	RABIA HAMEED
Supervisor	Prof. GONGMING YU
University	Harbin Engineering University, China

# Presentation Outline



**1.**

Introduction

**2.**

Methodology and  
Software

**3.**

Single and Double  
Diffractive  
Dilepton and Photon  
Production

**4.**

Results,  
Conclusion  
and  
References

**5.**

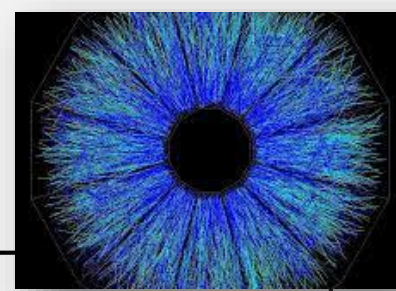
Future work

# 01 Introduction





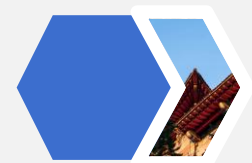
# 01 Introduction



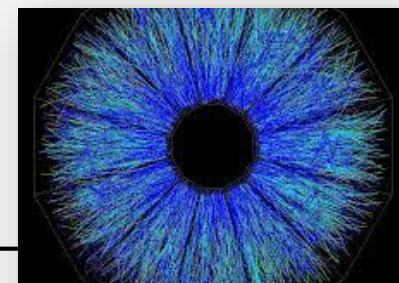
In high-energy,

at the Relativistic Heavy Ion Collider (RHIC) and the Large Hadron Collider (LHC), dileptons (di-electron and dimuon pairs) and photons arise in complex single- and double-diffractive processes. Diffractive processes offer an exceptional perspective to examine the underlying dynamics of strong interactions at extremely high energies.

The study measures cross-sections for dilepton production at LHC, analyzes the kinematic distributions of produced dileptons, and quantifies photon production rates in diffractive events. The technical goals include the invention of theoretical models and computational tools, advancement of detection and analysis techniques, and improvement of techniques for distinguishing and classifying diffractive events in high-energy collisions with complicated backgrounds.



# 01 Introduction



Study investigates the single and double diffractive production of dileptons and photons in ultra-peripheral collisions at the Large Hadron Collider (LHC). Utilizing advanced theoretical models that integrate quantum electrodynamics (QED) and Quantum Chromodynamics (QCD) frameworks, we analyze the differential cross sections of these processes, with particular emphasis on the role of the Pomeron and resolved Pomeron structures. Our research employs semi-coherent two-photon production mechanisms to predict dilepton production rates under various LHC energy scenarios. Our results demonstrate distinct production patterns for single and double diffractive processes, highlighting their potential as probes for studying the electromagnetic structure of heavy ions and the dynamics of soft interactions in high-energy collisions.

This paper provides new insights into the photon-mediated and Pomeron-mediated production mechanisms and sets the stage for future experimental investigations at collider facilities



## Main Contents:

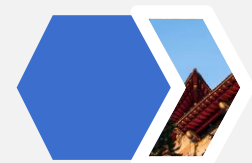
- **Diffractive processes** involve the exchange of momentum and energy with minimal disruption to the internal structure of particles.
- **Single diffractive production** results from a single quantum exchange, leading to the production of particles in the final state with minimal disturbance to their intrinsic properties.
- **Double diffractive production** involves the exchange of two quanta, yielding two distinct sets of particles, and providing a multifaceted view of particle interactions. Within single and double diffractive production, the focus on dileptons (electron and muon pairs) and photons are particularly intriguing.
- **Dileptons** are valuable probes for understanding electroweak interactions due to their charge and mass properties.
- **Photons,** as mediators of electromagnetic energy, offer valuable insights into quantum electrodynamics.

The research also aims to improve theoretical diffractive process models by including recent collision energies and creating and verifying computer programs by using a software (Mathematica) for finding the visual results to model diffractive dilepton and photon generation. Also, the study aims to investigate the proton structure and Parton Distribution Functions (PDF), as well as the implications for physics beyond the standard model.

# 02

## Methodology and Software





# METHODOLOGY

Methods used in this research field involves:

- **The Application Of Perturbative Quantum Chromodynamics (pQCD)**
- **Factorization Theory**
- **Parton Distribution Functions (Pdfs)**
- **Perturbative Techniques**
- **The Resolved Pomeron**
- **Photon Models**

- **Software**  
**(Mathematica)**

Techniques:	Usage:
Large Hadron Collider LHC	Study of high-energy particle collisions
Perturbative quantum chromodynamics (pQCD), factorization theory	To calculate the cross-sections for the production of dileptons in single and double diffractive processes.
High-energy particle collisions	Understanding the fundamental properties of matter and the universe.
Parton distribution functions (PDFs)	Describe the probability of finding a parton with a certain momentum fraction inside the hadron or photon.
Perturbative techniques	Calculate the short-distance contributions to the scattering process.
Resolved pomeron and photon models	Describe the partonic structure of the pomeron and photon.



## Factorization Theory:

In QCD, the factorization theorem allows the separation of the cross-section into parts that describe different scales of the interaction. These parts are typically:

**Parton Distribution Functions (PDFs):** Describes the probability of finding a parton (quark or gluon) with a certain fraction of the hadron's momentum.

**Hard Scattering Cross-section:** Describes the short-distance interaction of the partons.

## Quantum Chromodynamics (QCD):

QCD is the theory of the strong interaction, which are the fundamental constituents of matter. It is a type of quantum field theory based on the gauge group  $SU(3)$ .

**Confinement:** A key feature of QCD is confinement, which means that quarks and gluons are never found in isolation but always within hadrons.

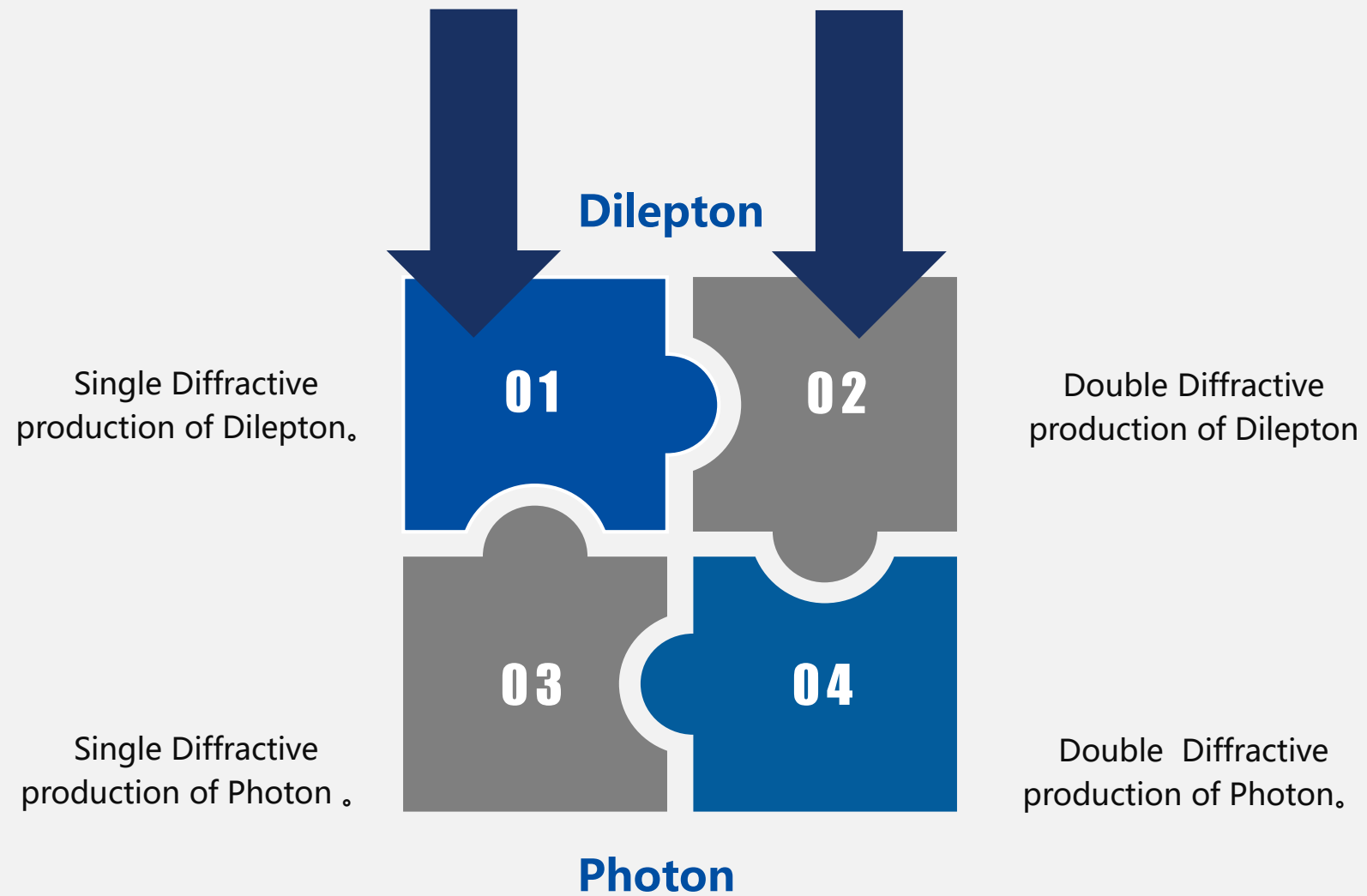
**Asymptotic Freedom:** At very short distances or high energies, the strong interaction becomes weaker, allowing quarks and gluons to behave almost as free particles.

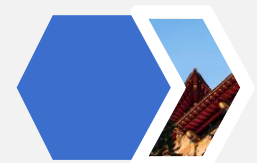
**Non-perturbative Effects:** QCD includes non-perturbative phenomena such as confinement and chiral symmetry breaking, which cannot be described by perturbation theory alone.

# 03

## Single and Double Diffractive Production of Dilepton and Photon at LHC







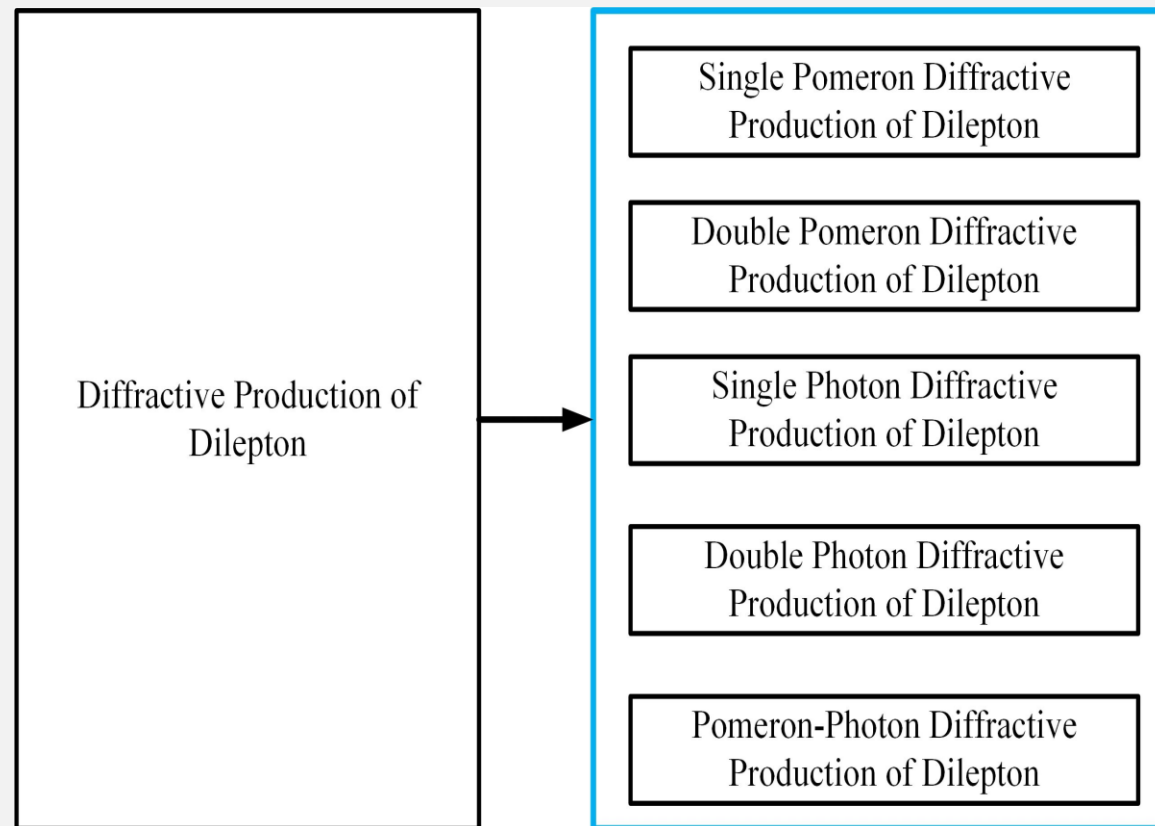
## Diffractive production of dileptons

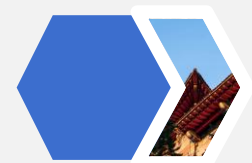
Diffractive production of dileptons in high-energy physics involves the generation of a pair of leptons in a diffractive process, such as those between protons at high-energy colliders like the Large Hadron Collider (LHC). These processes are characterized by the exchange of a Pomeron or a photon, leading to a final state with distinctive features, such as rapidity gaps and often the survival of initial state particles, such as protons, in a largely unaltered state. There are three mechanisms of diffractive dilepton production:

- Pomeron-Induced Dilepton Production,
- Photon-Induced Dilepton Production, and
- Pomeron-Photon Interactions.

Pomeron-Induced Dilepton Production involves the exchange of a colorless, gluonic entity, which can interact with quarks within a proton to produce dileptons through quark-antiquark annihilation or gluon fusion processes. Photon-Induced Dilepton Production occurs through the interaction of quasi-real photons emitted by colliding protons. Here is the flowchart of this chapter, first defined for dilepton.

## It Contains





# Derivation

As long diffractive processes are concerned, in hadron collisions they are well described, with respect to the overall cross sections, by Regge theory in terms of the exchange of a Pomeron with vacuum quantum numbers.

□ The Pomeron-nucleon coupling vertex is derived from the fundamental theory of strong interaction, QCD. Pomeron-Nucleon Coupling Vertex is a function representing the interaction between a Pomeron ( $\mathbb{P}$ ) and a nucleon (N, typically a proton or neutron).

□ In Regge theory, the Pomeron is a trajectory rather than a particle, representing a family of exchanged particles that dominate at high energies.

□ The Pomeron flux factor, the parton distribution functions for both proton and nucleus, and the Pomeron trajectory will all contribute to determining the probability and kinematics of the process.

Starting with the form factor equation and pomeron trajectory. The proposal of a phenomenological Pomeron exchange model with a vector-type Pomeron-nucleon vertex has been made;

$$V^{P-N} = \beta \gamma^\mu F_1(\hat{t})$$

$$F_1(\hat{t}) = \frac{4m_p^2 - A_P(\hat{t})}{(4m_p^2 - \hat{t}) \left(1 - \frac{\hat{t}}{B_P}\right)^{-2}}$$

According to the Regge theory, the Pomeron trajectory,  $\alpha_{\mathbb{P}}(\hat{t})$ ,

$$\alpha_{\mathbb{P}}(\hat{t}) = \alpha_{\mathbb{P}}(0) + \alpha'_{\mathbb{P}} t$$

*Values Used;*

$$\epsilon = 0.085, \alpha'_{\mathbb{P}} = 0.25 \text{ GeV}^{-2}$$

$$\alpha_{\mathbb{P}}(0) = 0.085, \alpha'_{\mathbb{P}} = 0.25 \text{ GeV}^{-2}, \alpha_{\mathbb{P}}(\hat{t}) \simeq 1.08 + 0.25(\hat{t})$$

$$m_p = 1.67 \times 10^{-27} \text{ kg.}$$

$$A_p = 2.8, B_p = 0.7, \beta = 3.24 \text{ GeV}^2.$$



# Derivation

- ❖ The parton distribution function PDF for proton is;

$$f_{\frac{\mathbb{P}}{p}}(x, Q^2) = \frac{9\beta^2}{4\pi^2} \left(\frac{1}{x}\right)^{2\alpha_{\mathbb{P}}(\hat{t})-1} [F_1(\hat{t})]^2$$

- ❖ The parton distribution function for nucleus

$$f_{\frac{\mathbb{P}}{N}}(x, Q^2) = \left(\frac{3A\beta_0 Q_0^2}{2\pi}\right) \left(\frac{\hat{s}}{m_p^2}\right) \frac{1}{x} e^{-x^2 M_N^2 / Q_0^2}$$

- ❖ The quark distribution function is given by:

$$f_{\frac{q}{\mathbb{P}}}(x) = A_1 x^{A_2} (1-x)^{A_3}$$

- ❖ The gluon distribution function is given by:

$$f_{\frac{g}{\mathbb{P}}}(x) = B_1 x^{B_2} (1-x)^{B_3}$$

Values Used;

$A_1=0.066$ ,  $A_2=0.29$ , and  $A_3=0.72$ .  
 $B_1=1.22$ ,  $B_2=3.13$  and,  $B_3=0.31$ .

- ❖ Also, parton distribution function for the nucleus  $f_N(x)$  combines the parton distributions of protons and neutrons within the nucleus, weighted by their relative numbers.

$$f_N(x) = R(x, A) \left[ \frac{Z}{A} f_P(x) + \frac{N}{A} f_n(x) \right]$$

- ❖ The function  $R(x, A)$  contain:

$$\begin{aligned} R(x, A) &= 1 + 1.19 \ln^{\frac{1}{6}} A [x^3 - 1.5(x_o + x_L)x^3 + 3x_o x_L x] \\ &\quad - \left[ \alpha_A \frac{1.08(A^{\frac{1}{3}} - 1)}{\ln(A + 1)} \sqrt{x} \right] e^{-x^2/x_o^2} \end{aligned}$$

- ❖ The parton distribution function of the nucleon:

$$xf(x) = A_0 x^{A_1} (1-x)^{A_2}$$

Values Used;

$\beta_0$  is the quark-nucleon coupling.

$Q_0 = 60.0 \text{ GeV}$ ,  $\beta_0 = 1.8 \text{ GeV}^{-1}$ .

The exponential term  $e^{-x^2 M_N^2 / Q_0^2}$  accounts for the spatial distribution of partons.

$x_o = 0.1$ ,  $x_L = 0.7$ ,  $\alpha_A = 0.1(A^{\frac{1}{3}} - 1)$ .





## Single Pomeron diffractive production process for dilepton

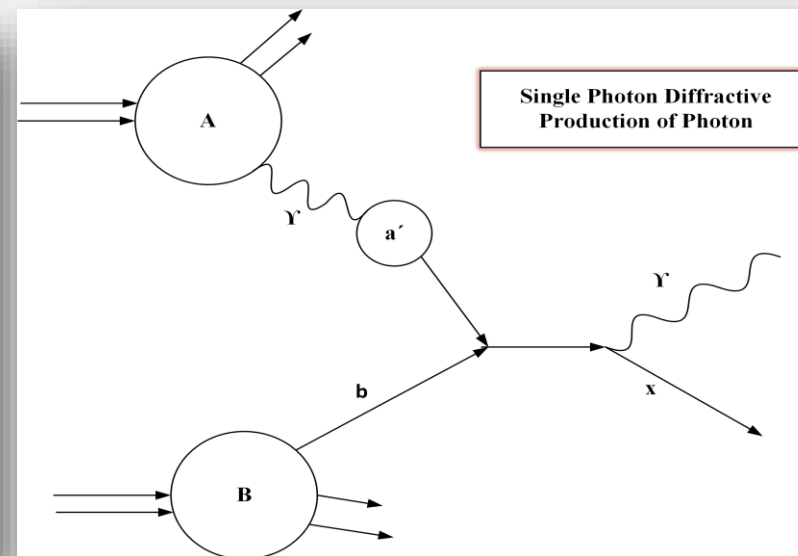
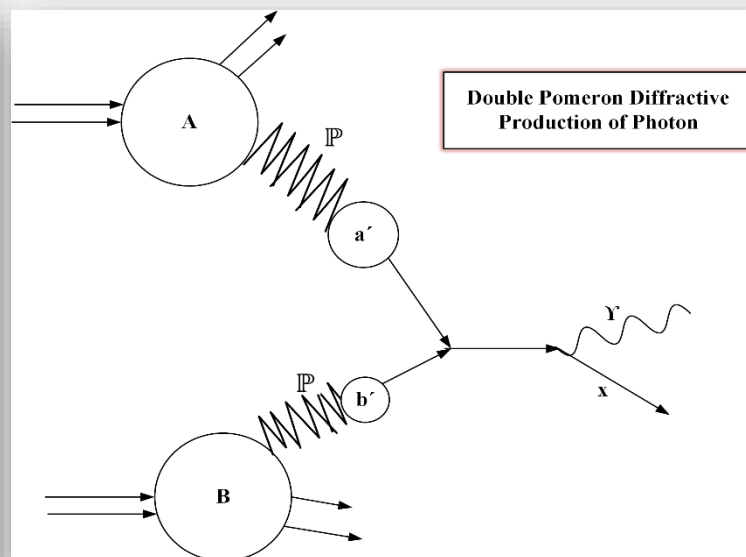
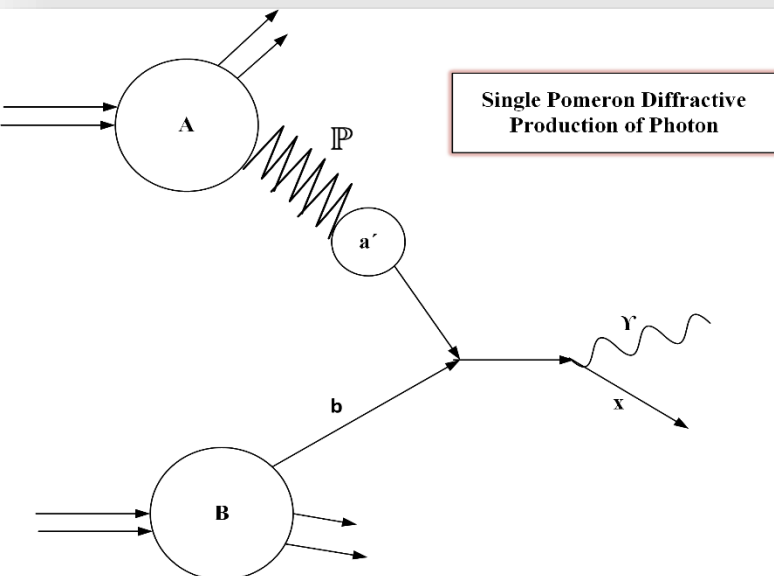
$$\frac{d\sigma_{AB \rightarrow l^+ l^- X}^{\text{Sin.Pom.Diff}}}{dM^2} = dx_a dz_a dx_b d\hat{t} f_{\frac{IP}{A}}(x_a, Q^2) f_{\frac{a'}{IP}}(z_a, \mu_F^2) f_{\frac{b}{B}}(x_b, Q^2) \frac{d\hat{\sigma}}{dM^2 d\hat{t}}(a' b \rightarrow l^+ l^- X) \rightarrow \text{(i)}$$

## Double Pomeron diffractive production processes for dilepton

$$\frac{d\sigma_{AB \rightarrow l^+ l^- X}^{\text{Dou.Pom.Diff}}}{dM^2} = dx_a dz_a dx_b dz_b d\hat{t} f_{\frac{IP}{A}}(x_a, Q^2) f_{\frac{a'}{IP}}(z_a, \mu_F^2) f_{\frac{IP}{B}}(x_b, Q^2) f_{\frac{b}{IP}}(z_b, \mu_F^2) \times \frac{d\hat{\sigma}}{dM^2 d\hat{t}}(ab \rightarrow l^+ l^- X) \rightarrow \text{(ii)}$$

## Single-photon diffractive production for dilepton

$$\frac{d\sigma_{AB \rightarrow l^+ l^- X}^{\text{Sin.Pho.Diff}}}{dM^2 dp_T^2 dy} = \int dx_a dx_b f_{\frac{\gamma}{A}}(x_a, Q^2) f_{\frac{a'}{\gamma}}(z_a, \mu_F^2) f_{\frac{b}{B}}(x_b, Q^2) \frac{x_a z_a x_b}{x_a x_b - x_a x_2} \times \frac{\alpha}{3\pi M^2} \sqrt{1 - \frac{4m_l^2}{M^2}} \left(1 + \frac{2m_l^2}{M^2}\right) \frac{d\hat{\sigma}}{d\hat{t}}(a' b \rightarrow \gamma^* X) \rightarrow \text{(iii)}$$



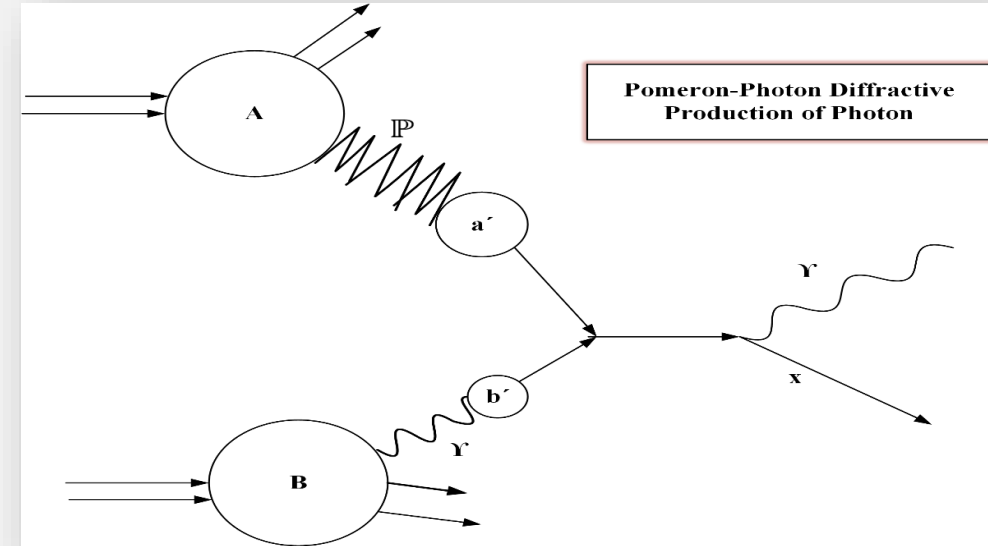
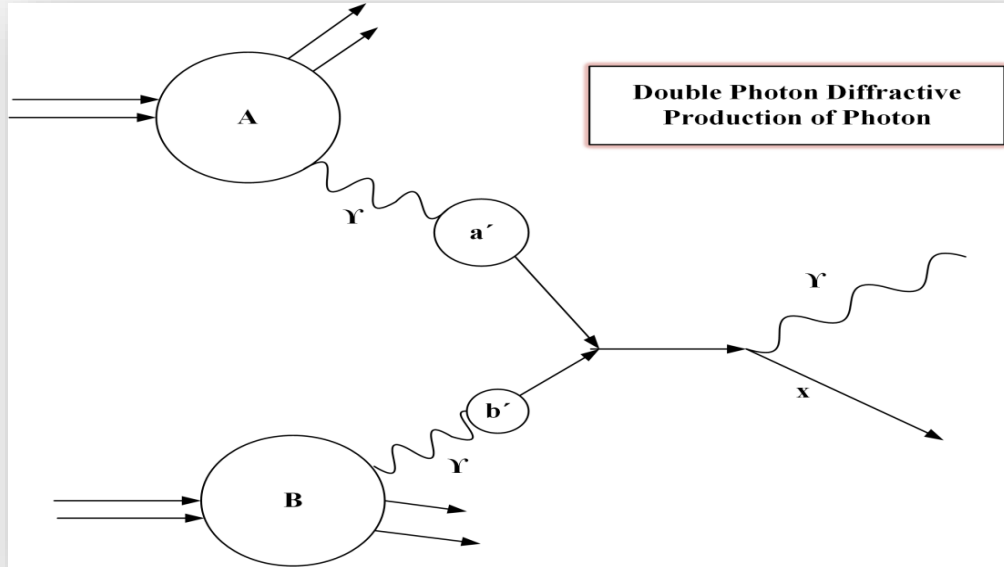


## Double-photon (photon-photon) diffractive production for dilepton:

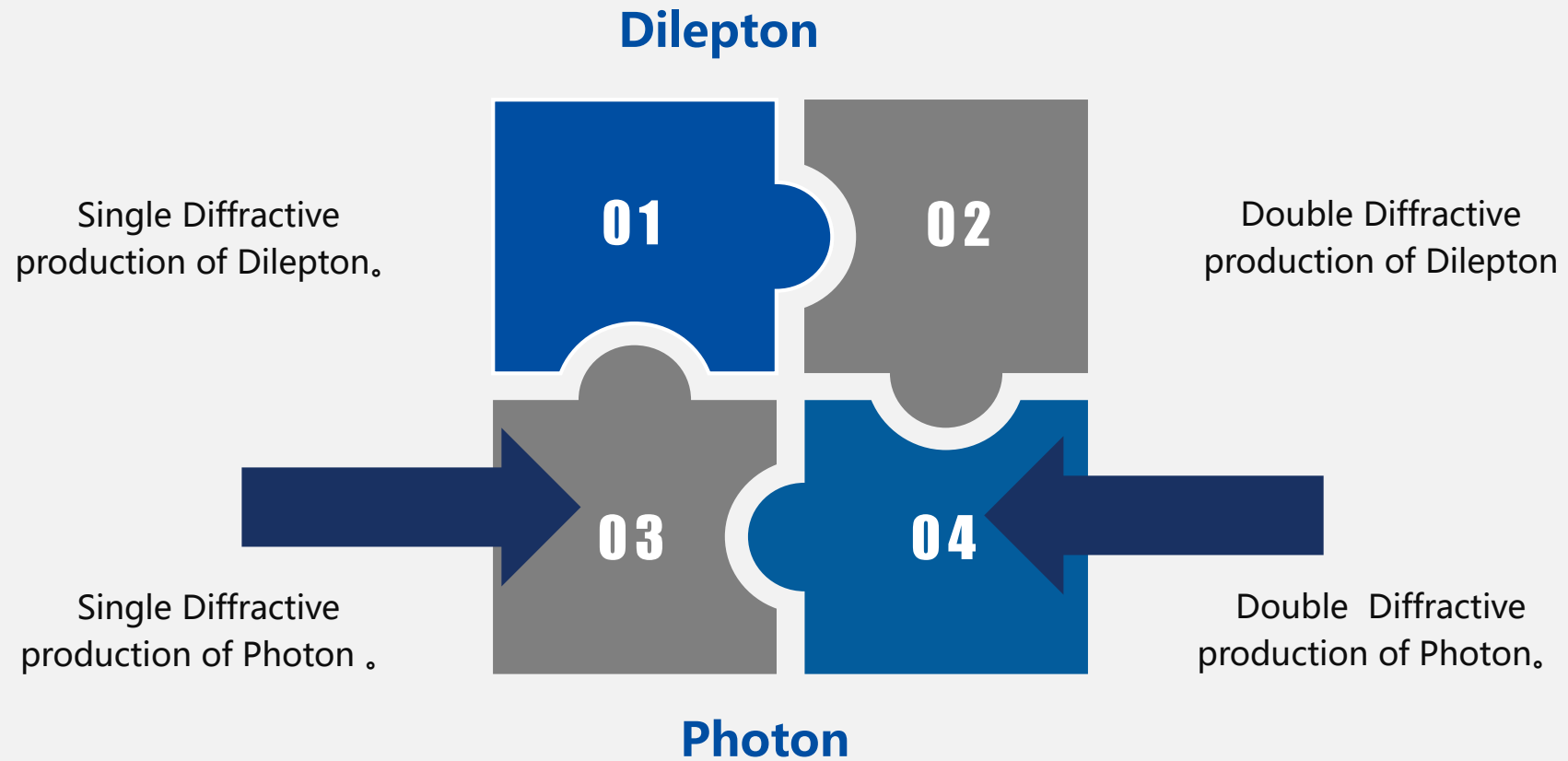
$$\frac{d\sigma_{AB \rightarrow l^+ l^- X}^{\text{Dou. Pho. Diff}}}{dM^2 dp_T^2 dy} = \int dx_a dx_b dz_b f_{\frac{\gamma}{A}}(x_a, Q^2) f_{\frac{a'}{\gamma}}(z_a, Q^2) f_{\frac{\gamma}{B}}(x_b, Q^2) f_{\frac{b'}{\gamma}}(z_b, Q^2) \times \frac{x_a z_a x_b z_b}{x_a x_b z_b - x_a x_2} \frac{\alpha}{3\pi M^2} \sqrt{1 - \frac{4m_l^2}{M^2}} \left(1 + \frac{2m_l^2}{M^2}\right) \frac{d\hat{\sigma}}{d\hat{t}}(a' b' \rightarrow \gamma^* X) \rightarrow \text{(iv)}$$

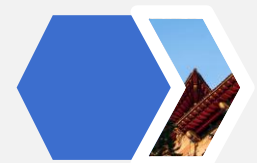
## Pomeron-photon associated diffractive production for dilepton:

$$\frac{d\sigma_{AB \rightarrow l^+ l^- X}^{\text{Pho. Pom. Diff}}}{dM^2 dp_T^2 dy} = \int dx_a dx_b dz_b f_{\frac{IP}{A}}(x_a, Q^2) f_{\frac{a'}{IP}}(z_a, \mu_F^2) f_{\frac{\gamma}{B}}(x_b, Q^2) f_{\frac{b'}{\gamma}}(z_b, Q^2) \times \frac{x_a z_a x_b z_b}{x_a x_b z_b - x_a x_2} \frac{\alpha}{3\pi M^2} \sqrt{1 - \frac{4m_l^2}{M^2}} \left(1 + \frac{2m_l^2}{M^2}\right) \frac{d\hat{\sigma}}{d\hat{t}}(a' b' \rightarrow \gamma^* X) \rightarrow \text{(v)}$$









## Diffractive production of Photon

In order to move forward to describe the diffractive production for photon. Here, is a layout as shown →

It include the diffractive production of photon mainly in five steps. These are single pomeron and double pomeron diffractive production of photon, single photon and double photon production of photon, and on the last pomeron-photon diffractive production of photon.

Diffractive Production of Photon

Single Pomeron Diffractive  
Production of Photon

Double Pomeron Diffractive  
Production of Photon

Single Photon Diffractive  
Production of Photon

Double Photon Diffractive  
Production of Photon

Pomeron-Photon Diffractive  
Production of Photon



## Single pomeron diffractive production processes for photon

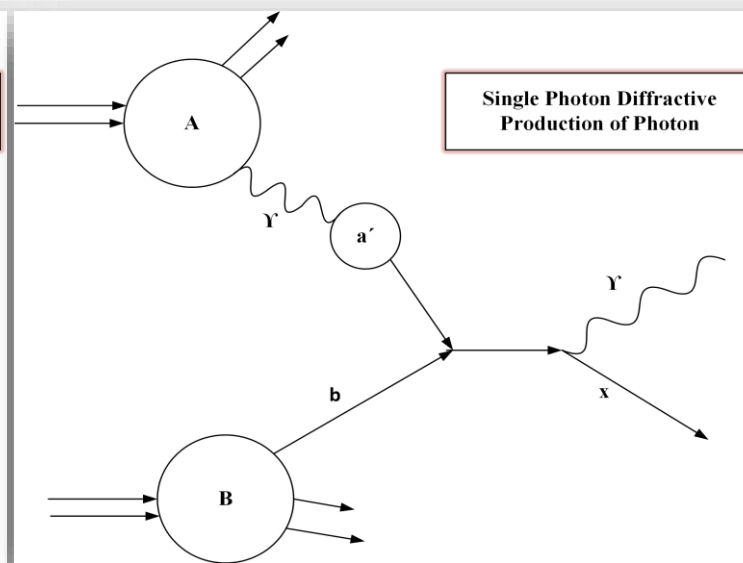
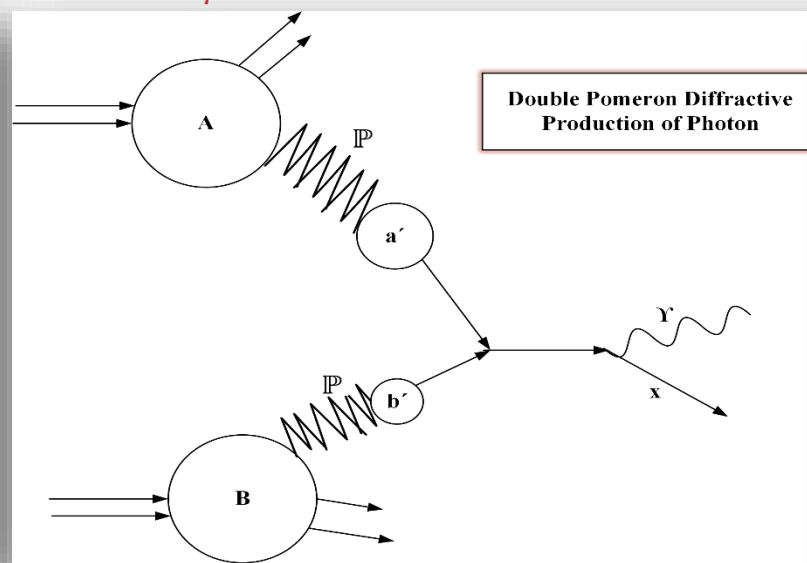
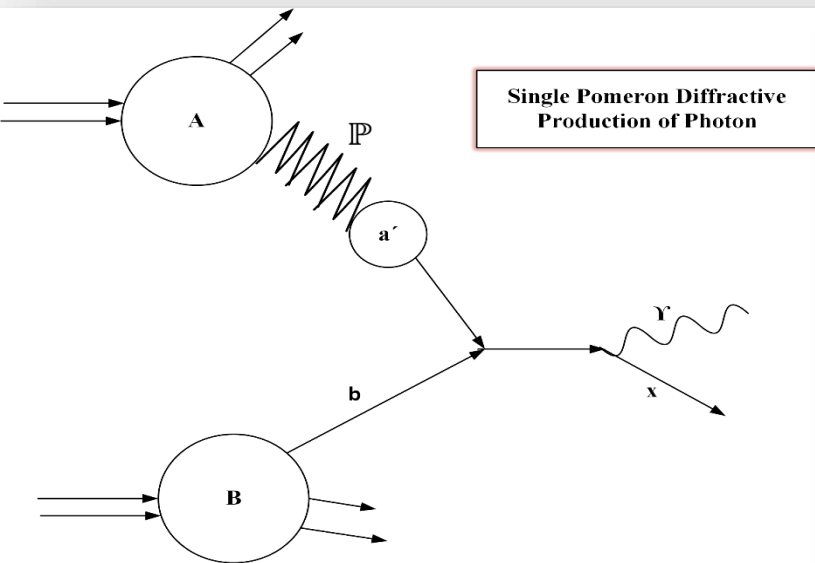
$$\frac{d\sigma_{AB \rightarrow \gamma X}^{\text{Sin.Pom.Diff}}}{dp_T^2 dy} = \int dx_a dx_b f_{\frac{IP}{A}}(x_a, Q^2) f_{\frac{a'}{IP}}(z_a, \mu_F^2) f_{\frac{b}{B}}(x_b, Q^2) \frac{x_a z_a x_b}{x_a x_b - x_a x_2} \frac{d\hat{\sigma}}{d\hat{t}}(a' b \rightarrow \gamma X) \rightarrow (\text{vi})$$

## Double pomeron diffractive production processes for photon

$$\frac{d\sigma_{AB \rightarrow l^+ l^- X}^{\text{Dou.Pom.Diff}}}{dp_T^2 dy} = \int dx_a dx_b dz_b f_{\frac{IP}{A}}(x_a, Q^2) f_{\frac{a'}{IP}}(z_a, \mu_F^2) f_{\frac{IP}{B}}(x_b, \mu_F^2) f_{\frac{b'}{IP}}(z_b, \mu_F^2) \times \frac{x_a z_a x_b z_b}{x_a x_b z_b - x_a x_2} \frac{d\hat{\sigma}}{d\hat{t}}(a' b' \rightarrow \gamma X) \rightarrow (\text{vii})$$

## Single-photon diffractive production for photon

$$\frac{d\sigma_{AB \rightarrow \gamma X}^{\text{Sin.Pho.Diff}}}{dp_T^2 dy} = \int dx_a dx_b f_{\frac{\gamma}{A}}(x_a, Q^2) f_{\frac{a'}{\gamma}}(z_a, \mu_F^2) f_{\frac{b}{B}}(x_b, Q^2) \frac{x_a z_a x_b}{x_a x_b - x_a x_2} \frac{d\hat{\sigma}}{dM^2 d\hat{t}}(a' b \rightarrow \gamma X) \rightarrow (\text{viii})$$



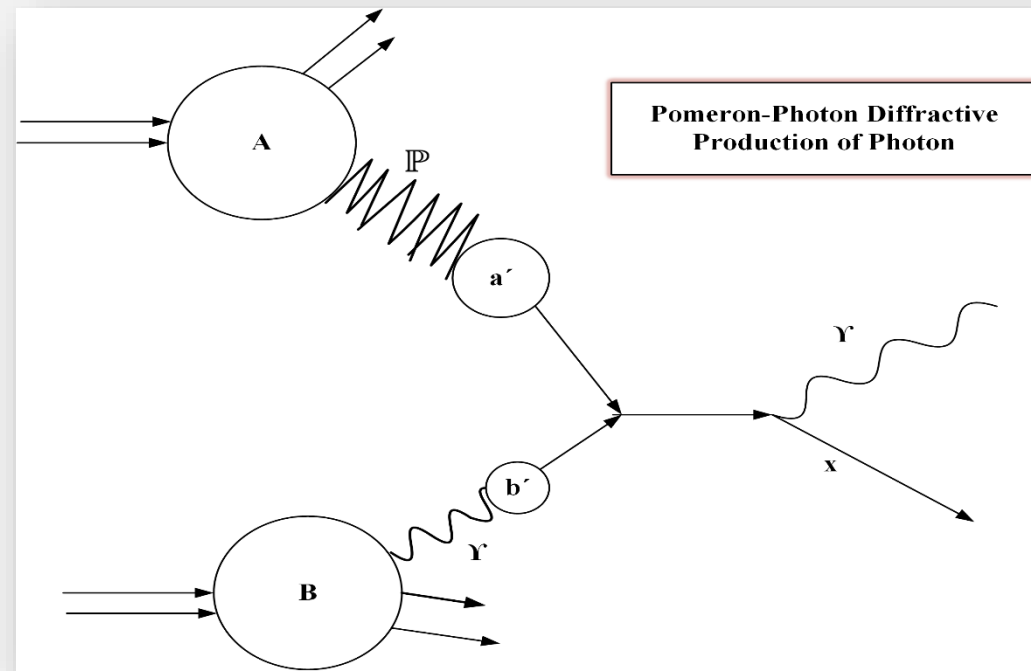
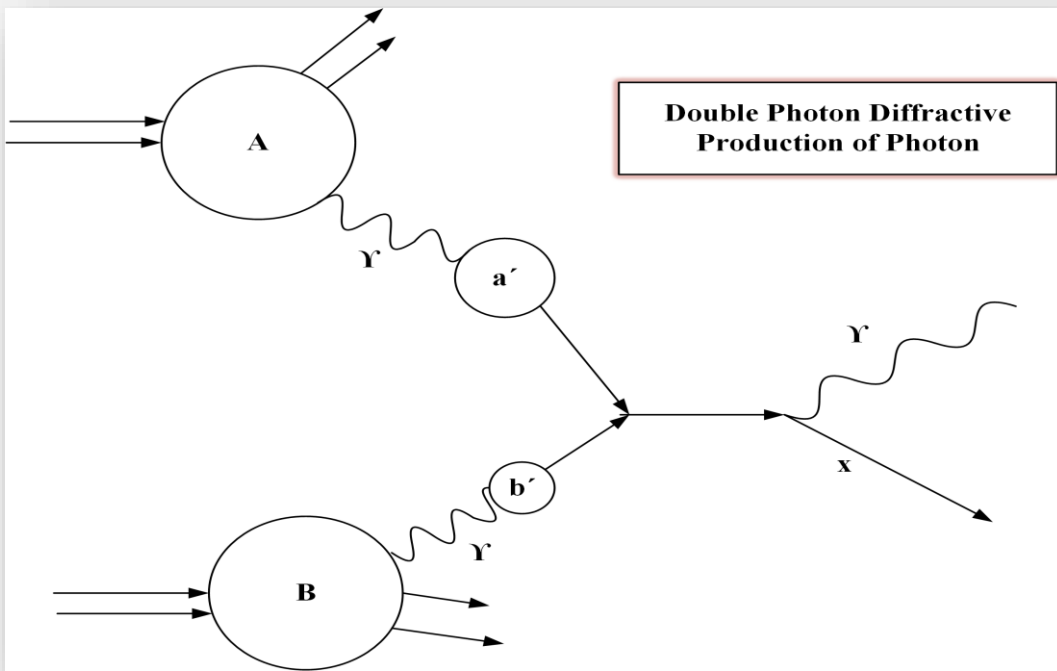


## Double-photon (photon-photon) diffractive production for photon

$$\frac{d\sigma_{AB \rightarrow l^+ l^- X}^{\text{Dou. Pho. Diff}}}{dp_T^2 dy} = \int dx_a dx_b dz_b f_{\frac{\gamma}{A}}(x_a, Q^2) f_{\frac{a'}{\gamma}}(z_a, Q^2) f_{\frac{\gamma}{B}}(x_b, Q^2) f_{\frac{b'}{\gamma}}(z_b, Q^2) \times \frac{x_a z_a x_b z_b}{x_a x_b z_b - x_a x_2} \frac{d\hat{\sigma}}{d\hat{t}}(a' b' \rightarrow \gamma X) \rightarrow (\text{ix})$$

## Pomeron-photon associated diffractive production for photon

$$\frac{d\sigma_{AB \rightarrow l^+ l^- X}^{\text{Pho. Pom. Diff}}}{dp_T^2 dy} = \int dx_a dx_b dz_b f_{\frac{IP}{A}}(x_a, Q^2) f_{\frac{a'}{IP}}(z_a, \mu_F^2) f_{\frac{\gamma}{B}}(x_b, Q^2) f_{\frac{b'}{\gamma}}(z_b, Q^2) \times \frac{x_a z_a x_b z_b}{x_a x_b z_b - x_a x_2} \frac{d\hat{\sigma}}{d\hat{t}}(a' b' \rightarrow \gamma X) \rightarrow (\text{x})$$





## Summary

These numerical calculations provides an in-depth exploration of diffractive processes. The diffractive production processes in particle physics involve the creation of either dileptons (a lepton and its corresponding antiparticle) or photons. There are three main types of diffractive production processes: Single pomeron, double pomeron, and single photon.

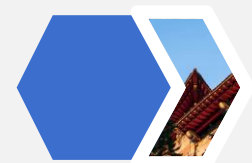
For dileptons, a single pomeron leads to the production of a dilepton pair through the decay of an intermediary particle like a virtual photon. For photons, a single photon is produced directly through diffractive scattering. For double photons, two photons from interacting hadrons collide and produce a dilepton pair through a quantum electro-dynamical process. For photons, this scenario involves two photons interacting to produce another photon, which is not a standard process. Pomeron-photon diffractive production involves a pomeron and a photon from different hadrons interacting, leading to the production of a dilepton pair.

For photons, a pomeron-photon interaction results in the production of a photon, likely due to the electromagnetic interaction from the incoming photon. These processes differ in their processes and their underlying mechanisms. In short, the distinction between these processes lies in the types of particles exchanged (pomerons or photons) and the final state particles produced (dilepton pairs or photons). The processes involving dilepton production are typically mediated by virtual photons, while those producing photons directly involve electromagnetic interactions. The conservation of quantum numbers, energy, and momentum is crucial in all these interaction.

# 04

## Results and Discussion





# Diffractive production process for dilepton

This section will feature graphical representations to illustrate the dependence of the cross-section on variables such as the invariant mass of the dilepton system and momentum fractions, alongside the kinematic distributions like rapidity and transverse momentum of the produced dileptons.



Pb-Pb	A=208	Z=82	$\sqrt{s_{NN}}=5.02\text{TeV}$
P-Pb	A=208	Z=82	$\sqrt{s_{NN}}=8.16\text{TeV}$
P-p	A=1	Z=1	$\sqrt{s_{NN}}=7\text{TeV} \text{ \& } 13\text{TeV}$

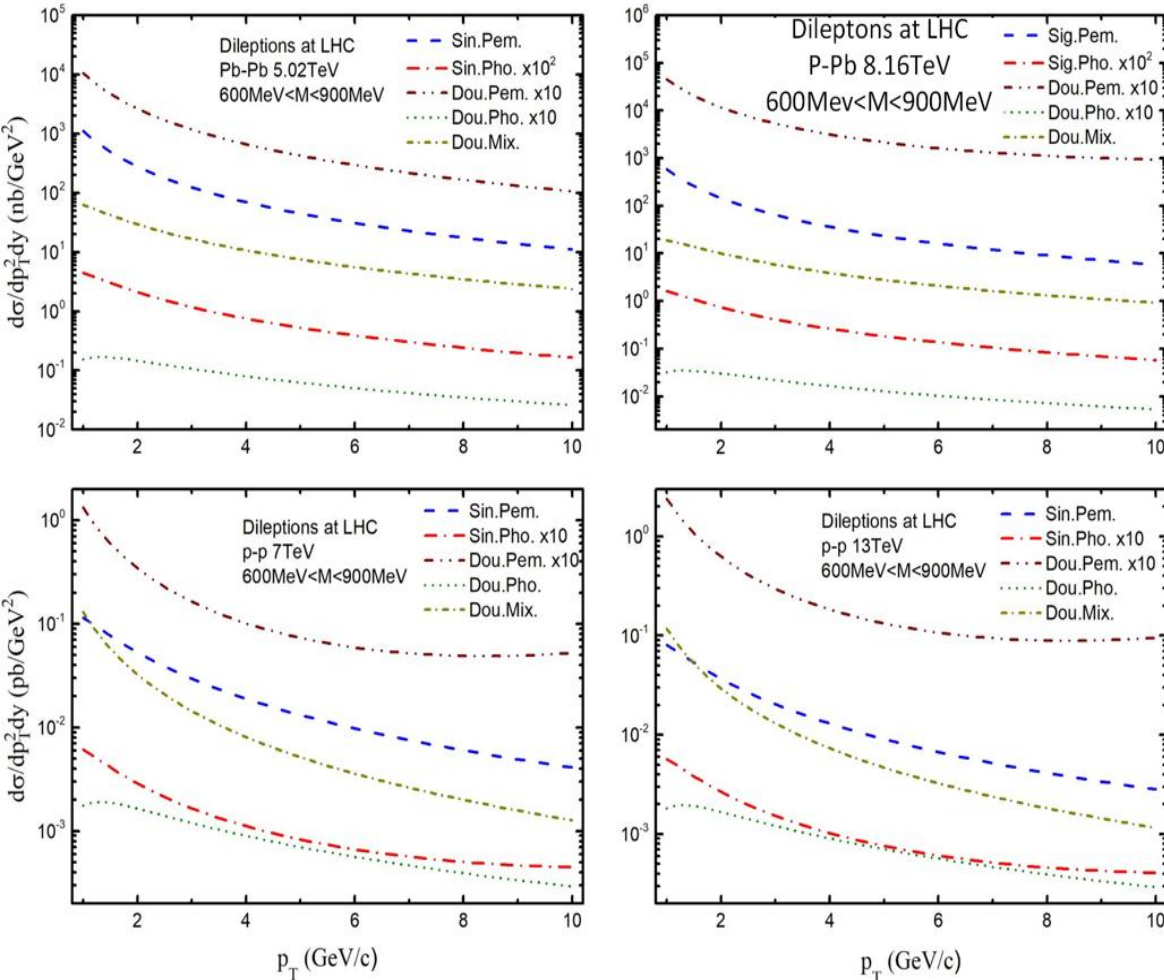
The cross-sections diminish with an increase in transverse momentum ( $p_T$ ), which is a characteristic trend expected from diffractive scattering phenomena. The y-axis shows the differential cross-section ( $d\sigma/dp_T^2 dy$ ) which measures how often particles are produced at a certain transverse momentum ( $p_T$ , shown on the x-axis) and rapidity ( $y$ ).

- [Sin.Pem.](#) The solid lines (blue) indicate this process and it's typically the baseline for comparison.
- [Sin.Pho.](#) This process is depicted with dotted lines (red) and scaled by a factor for visibility (e.g., x10), given that photon exchange processes are less probable than pomeron exchanges.
- [Dou.Pem.](#) The dashed lines (brown) show this process, which is generally rarer than single diffractive processes and therefore often scaled up by a significant factor (e.g., x10) to be visible on the same scale.
- [Dou.Pho.](#) The dot-dashed lines (sea-foam green) represent this.
- [Dou.Mix.](#) This might represent a mixed double exchange involving both pomeron and photon exchanges. The fine dotted lines (olive green) depict this process.



# Diffractive production process for dilepton

- Top Left: Pb-Pb collisions at  $\sqrt{s_{NN}} = 5.02$  TeV
- Top Right: p-Pb collisions at  $\sqrt{s_{NN}} = 8.16$  TeV
- Bottom Left: p-p collisions at  $\sqrt{s_{NN}} = 7$  TeV
- Bottom Right: p-p collisions at  $\sqrt{s_{NN}} = 13$  TeV



## (1) Pb-Pb 5.02 TeV

The hierarchy of processes by the size of their cross-sections is as follows:

- Single Photon (Sin Pho) production has the lowest cross-section.
- Double Photon (Dou Pho) production is higher than single photon production.
- Mixed Double (Dou Mix) exchange is greater than double photon production.
- Single Pomeron (Sin Pem) and Double Pomeron (Dou Pem) are approximately equal and have the highest cross-sections among the processes considered.

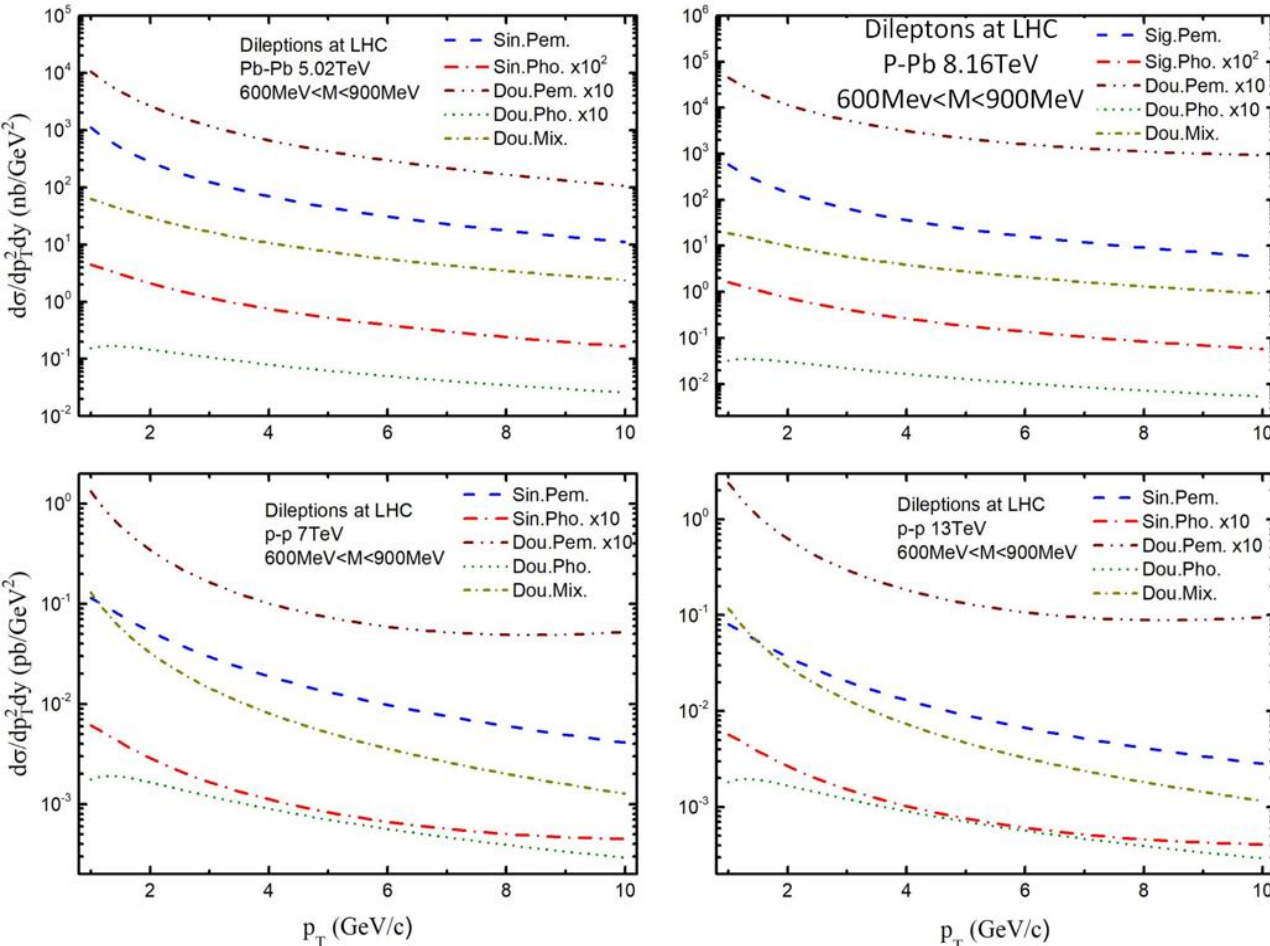
## (2) p-Pb 8.16 TeV

The ordering is similar to Pb-Pb collisions, with the distinction that Double Pomeron (Dou Pem) production has a larger cross-section than Single Pomeron (Sin Pem) production.



# Diffractive production process for dilepton

- Top Left: Pb-Pb collisions at  $\sqrt{s_{NN}} = 5.02$  TeV
- Top Right: p-Pb collisions at  $\sqrt{s_{NN}} = 8.16$  TeV
- Bottom Left: p-p collisions at  $\sqrt{s_{NN}} = 7$  TeV
- Bottom Right: p-p collisions at  $\sqrt{s_{NN}} = 13$  TeV



## (3) p-p 7 TeV

The hierarchy is much the same as in Pb-Pb collisions, with Single Pomeron and Double Pomeron processes being nearly equal and the largest.

## (4) p-p 13 TeV

Again, Single Photon and Double Photon production have the lowest cross-sections, but here the Double Pomeron process becomes more dominant compared to the Single Pomeron process.

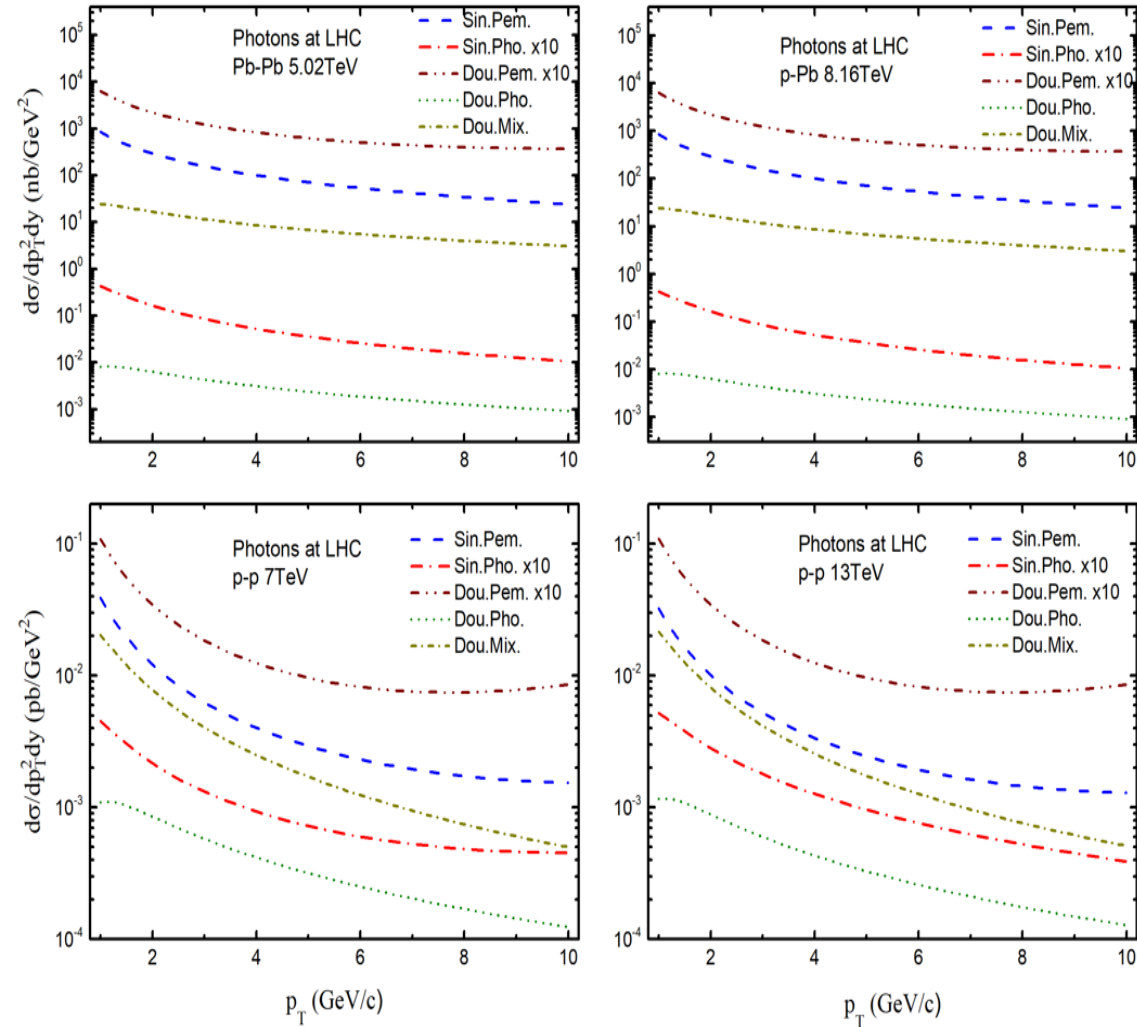
# Diffractive production process for Photon

## (1) Pb-Pb Collisions at 5.02 TeV

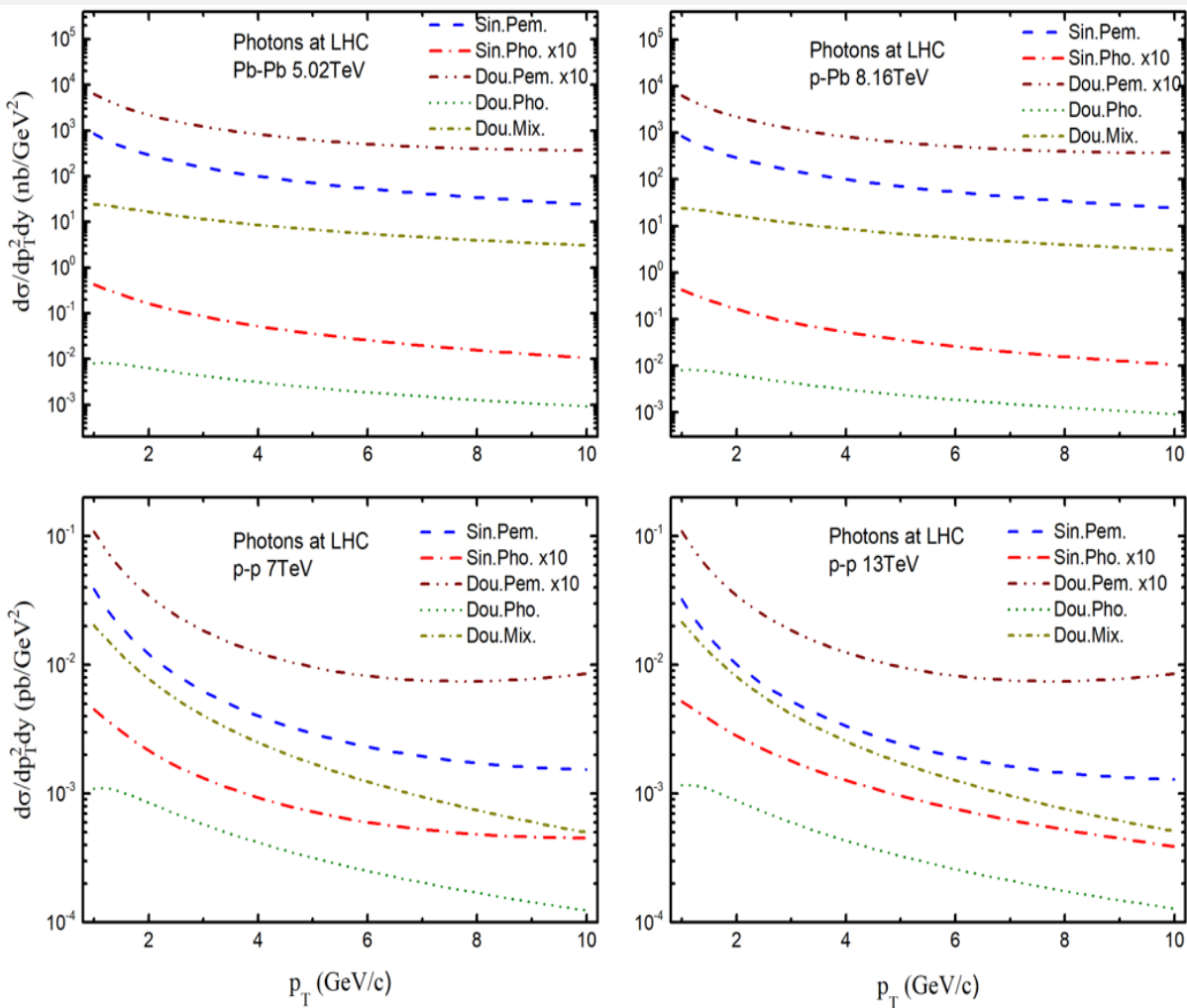
The single photon production process (Sin. Pho.) has the lowest cross-section. Double photon production (Dou. Pho.) has a higher cross-section than single photon production. The mixed double exchange process (Dou. Mix.) has a higher cross-section than double photon production. The single pomeron exchange (Sin. Pem.) and double pomeron exchange (Dou. Pem.) have similar cross-sections, which are the highest among the processes displayed.

## (2) p-Pb Collisions at 8.16 TeV

Single photon production (Sin. Pho.) remains the lowest. Double photon production (Dou. Pho.) has a higher cross-section. The mixed double exchange (Dou. Mix.) has a higher cross-section than both photon processes. Single pomeron exchange (Sin. Pem.) has a slightly smaller cross-section than double pomeron exchange (Dou. Pem.), which is the highest.



# Diffraction production process for Photon



## (3) p-p Collisions at 7 TeV

Single pomeron exchange (Sin. Pem.) has a larger cross-section than double pomeron exchange (Dou. Pem.).

## (4) p-p Collisions at 13 TeV

Single photon production (Sin. Pho.) continues to have the lowest cross-section. Double photon production (Dou. Pho.) has a higher cross-section than single photon production. The mixed double exchange (Dou. Mix.) has a higher cross-section than double photon production. Single pomeron exchange (Sin. Pem.) has a large cross-section than double pomeron exchange (Dou. Pem.).



## Comparative Observations

Overall, the two results for dilepton and photon contain differential cross-section plots for particle production at the Large Hadron Collider (LHC) for different collision systems and energies. The first result deals with dilepton production, and the second with photon production. Here's a combined summary of the observations from both:

### Dilepton Production:

- Cross-sections for all processes decrease with increasing  $p_T$ .
- For Pb-Pb at 5.02 TeV, the ordering from smallest to largest cross-section is: single photon, double photon, mixed double, single pomeron, and double pomeron.
- For p-Pb at 8.16 TeV and p-p at 13 TeV, the Double Pomeron has a larger cross-section compared to the Single Pomeron.
- For p-p at 7 TeV, Single Pomeron and Double Pomeron have similar cross-sections.
- Between Pb-Pb 5.02 TeV and p-Pb 8.16 TeV, the Double Pomeron becomes more pronounced.
- Between p-p 7 TeV and p-p 13 TeV, the Double Pomeron gains in significance as the energy increases.

### Photon Production:

- As in dilepton production, photon production cross-sections also decrease with increasing  $p_T$ .
- Across all energies and collision systems, the general hierarchy is consistent: Single Photon < Double Photon < Mixed Double < Single Pomeron  $\lesssim$  Double Pomeron.
- Double Pomeron exchange tends to increase in significance with increasing collision energy.



## Comparative Observations

In order to explain the combined conclusion for both dilepton and photon production at the LHC, there is a consistent pattern across different types of collisions (Pb-Pb, p-Pb, and p-p) and varying energies (5.02 TeV, 7 TeV, 8.16 TeV, and 13 TeV):

All processes show decreasing cross-sections with increasing  $p_T$ , reflecting the fundamental behavior of such high-energy collisions where high  $p_T$  events are less probable. Pomeron exchange processes (both Single and Double) generally have higher cross-sections compared to photon exchange processes. This suggests that strong interactions (possibly mediated by gluons in the case of pomerons) are dominant in these collision scenarios. The relative importance of Double Pomeron exchange grows with increasing energy, particularly in proton-proton collisions. This may indicate that as the energy available for the collisions increases, the probability of more complex interactions, like Double Pomeron exchanges, also increases.



# Conclusion

The conclusion of this research highlights the profound insights gained into the phenomena of ultraperipheral collisions (UPC) at high-energy heavy ion accelerators such as the RHIC and the LHC. By meticulously analyzing the photoproduction of dileptons and photons within these highly specialized Collision energies, this study has shed light on the intricate electromagnetic interactions and quantum dynamics that govern such processes. The aim of this research was to delve deep into the fundamental physics underlying UPCs, exploring the critical role of electromagnetic radiation in generating final states like dileptons and photons, and to elucidate the complex interplay between Quantum Electrodynamics (QED) and Quantum Chromodynamics (QCD) in these events. Focusing on the motion, angular distribution, and correlations in invariant mass of dilepton pairs, particularly through the lens of Pomeron exchange and the application of Regge theory and QCD-based factorization techniques, this study has not only unraveled the complex interactions at play but also provided predictive insights under various kinematic conditions. The use of the equivalent photon approximation method facilitated a streamlined approach to understanding the electromagnetic field's influence on the virtual photon flux, enabling a more manageable exploration of photon emission and absorption processes.



# Conclusion

The summary highlights the influence of energy levels and collision types on interaction cross-sections in high-energy particle physics. Higher energy collisions, like 13 TeV compared to 7 TeV in proton-proton (p-p) collisions, tend to increase the probability of parton interactions. For dileptons, the dominant process in dilepton production appears to be the double pomeron exchange (Dou. Pem.). This means that the interactions involving two pomeron exchanges are more prevalent than those with single pomeron exchange (Sin. Pem.), single photon exchange (Sin. Pho.), and other mixed or double processes. While for photons, in proton-proton (p-p) collisions, the double pomeron exchange (Dou. Pem.) is slightly less prevalent than single pomeron exchange (Sin. Pem.), particularly at higher transverse momentum ( $p_T$ ). In proton-lead (p-Pb) and lead-lead (Pb-Pb) collisions, the single pomeron exchange has a similar magnitude to that of the double pomeron exchange. However, as the transverse momentum increases, the single pomeron exchange is slightly less than the double pomeron exchange.

In proton-lead (p-Pb) and lead-lead (Pb-Pb) collisions, the single pomeron exchange has a similar magnitude to that of the double pomeron exchange. However, as the transverse momentum increases, the single pomeron exchange is slightly less than the double pomeron exchange. The results indicate that the study of dileptons and photons in ultra-peripheral heavy ion collisions are feasible at LHC energies. Insights gained will contribute to a deeper understanding of QCD in diffractive processes across varying energy regimes.





# References

1. Stroynowski, R., *Lepton pair production in hadron collisions*. Physics Reports, 1981. **71**(1): p. 1-50.
2. Baur, G., K. Hencken, and D. Trautmann, *Photon-photon and photon-hadron interactions at relativistic heavy ion colliders*. Progress in Particle and Nuclear Physics, 1999. **42**: p. 357-366.
3. Baur, G., K. Hencken, and D. Trautmann, *Photon-photon physics in very peripheral collisions of relativistic heavy ions*. Journal of Physics G: Nuclear and Particle Physics, 1998. **24**(9): p. 1657.
4. Buonocore, L., et al., *Photon and leptons induced processes at the LHC*. Journal of High Energy Physics, 2021. **2021**(12): p. 1-35.
5. Bourilkov, D., *Photon-induced background for dilepton searches and measurements in pp collisions at 13 TeV*. arXiv preprint arXiv:1606.00523, 2016.
6. Ingelman, G. and K. Prytz, *The Pomeron structure in DIS and gluon recombination effects*. Zeitschrift für Physik C Particles and Fields, 1993. **58**: p. 285-293.
7. Bartels, J. and G. Ingelman, *On the pomeron structure function in QCD*. Physics Letters B, 1990. **235**(1-2): p. 175-181.
8. Donnachie, S., et al., *Pomeron physics and QCD*. 2002: Cambridge University Press.
9. Kopeliovich, B., R. Pasechnik, and I. Potashnikova, *Diffraction dijet production: Breakdown of factorization*. Physical Review D, 2018. **98**(11): p. 114021.
10. McGaughey, P., J. Moss, and J.-C. Peng, *High-energy hadron-induced dilepton production from nucleons and nuclei*. Annual Review of Nuclear and Particle Science, 1999. **49**(1): p. 217-253.
11. Baltz, A., et al., *The physics of ultraperipheral collisions at the LHC*. Physics reports, 2008. **458**(1-3): p. 1-171.
12. Contreras, J. and J. Tapia Takaki, *Ultra-peripheral heavy-ion collisions at the LHC*. International Journal of Modern Physics A, 2015. **30**(08): p. 1542012.
13. Klein, S.R., *Photoproduction at RHIC and the LHC*. arXiv preprint arXiv:0810.3039, 2008.
14. Khoze, V., A. Martin, and M. Ryskin, *Dynamics of diffractive dissociation*. The European Physical Journal C, 2021. **81**(2): p. 1-14.
15. Levin, E., *An introduction to Pomerons*. arXiv preprint hep-ph/9808486, 1998.
16. Broilo, M., *Nonperturbative Dynamics of Hadronic Collisions*. arXiv preprint arXiv:1908.01040, 2019.
17. Donnachie, A. and P.V. Landshoff, *Hard diffraction: production of high pT jets, W or Z, and Drell-Yan pairs*. Nuclear Physics B, 1988. **303**(4): p. 634-652.
18. Boreskov, K., et al., *The partonic interpretation of reggeon theory models*. The European Physical Journal C, 2005. **44**: p. 523-531.
19. Kaidalov, A.B., *Pomeranchuk singularity and high-energy hadronic interactions*. Physics-Uspekhi, 2003. **46**(11): p. 1121.
20. Collins, P.D.B., *Regge theory and particle physics*. Physics Reports, 1971. **1**(4): p. 103-233.
21. Collins, P.D.B., *An introduction to Regge theory and high energy physics*. 1977: Cambridge University Press.
22. Hothi, N. and S. Bisht, *Insight of the relation between Regge theory and Hadron dynamics*. Indian Journal of Physics, 2021. **95**: p. 2829-2836.
23. Forshaw, J.R. and D.A. Ross, *Quantum chromodynamics and the pomeron*. 1997: Cambridge University Press.
24. Kopeliovich, B. and A. Rezaeian, *Applied high energy QCD*. International Journal of Modern Physics E, 2009. **18**(08): p. 1629-1696.
25. Kharzeev, D., *Quarkonium interactions in QCD*. Proc. Int. Sch. Phys. Fermi, 1996. **130**(arXiv: nucl-th/9601029): p. 105-131.
26. Kubasiak, G. and A. Szczurek, *Inclusive and exclusive diffractive production of dilepton pairs in proton-proton collisions at high energies*. Physical Review D, 2011. **84**(1): p. 014005.
27. Schäfer, W., G. Ślipek, and A. Szczurek, *Exclusive diffractive photoproduction of dileptons by timelike Compton scattering*. Physics Letters B, 2010. **688**(2-3): p. 185-191.
28. Ślipek, G., W. Schäfer, and A. Szczurek, *Diffractive photoproduction of lepton pairs at high energy*. in *Proceedings of the XVIIIth International Workshop on Deep-Inelastic Scattering and Related Subjects*. April 19-23. 2010.
29. Enterria, D. and J.-P. Lansberg, *Study of higgs boson production and its b-bbar decay in gamma-gamma processes in proton-nucleus collisions at the Lhc*. arXiv preprint arXiv:0909.3047, 2009.
30. Yu, G.-M., *Photoproduction of dileptons, photons, and light vector mesons in ultrarelativistic heavy ion collisions*. Physical Review C, 2015. **91**(4): p. 044908.



---

# Parameters used in derivations





**For the proton,**

the PDF is given by  $f_{IP}^P(x, Q^2)$  and is parameterized by the form factor  $F_1(t)$  of the nucleon.

$$F_1(\hat{t}) = \frac{4m_p^2 - A_P(\hat{t})}{(4m_p^2 - \hat{t}) \left(1 - \frac{\hat{t}}{B_P}\right)^{-2}}$$

where  $m_p$  = mass of the proton,  
 $A_P = 2.8$  and  $B_P = 0.7$

**For the nucleus,**

the PDF is denoted by  $f_{IP}^N(x, Q^2)$  and is parameterized by the pomeron flux factor  $\beta_0$  and the pomeron-nucleon coupling constant  $Q_0$ . The function of the energy  $\sqrt{s_{NN}}$  and the nuclear mass number  $A$ .  $M_N$  is the nucleon mass

$$f_{IP}^N(x, Q^2) = \left(\frac{3A\beta_0 Q_0^2}{2\pi}\right) \left(\frac{\hat{s}}{m_p^2}\right) \frac{1}{x} e^{-x^2 M_N^2 / Q_0^2}$$

In short, PDFs are calculated using pQCD and factorization theory, and are parameterized by the pomeron flux factor, the pomeron trajectory, the form factor of the nucleon, and the pomeron-nucleon coupling constant.

$$\hat{s} = x_{IP} x_b \sqrt{s_{NN}}, \quad Q_0 = 60.0 \text{ GeV}, \quad \beta_0 = 1.8 \text{ GeV}^{-1}, \quad \epsilon = 0.085$$

## • Partonic structure of pomeron and parton distribution function of the nucleus:

$$f_{\frac{q}{IP}}(x) = A_1 x^{A_2} (1-x)^{A_3}$$

$$f_{\frac{g}{IP}}(x) = B_1 x^{B_2} (1-x)^{B_3} \text{ Where;}$$

$$A_1=0.066, A_2=0.29, A_3=0.72, B_1=1.22, B_2=3.13, B_3=0.31$$

$f_{\frac{q}{IP}}(x) \rightarrow$  represent the probability of finding a quark

$f_{\frac{g}{IP}}(x) \rightarrow$  represent the probability of finding a gluon

### The parton distribution function of the nucleus,

It is given by the following equation:

$$\text{➤ } f_N(x) = R(x, A) \left[ \frac{Z}{A} f_P(x) + \frac{N}{A} f_n(x) \right]$$

$f_N(x) \rightarrow$  probability of finding a Parton, fraction of the nucleus momentum

Z and N are the numbers of protons and neutrons in the nucleus

$f_P(x) \rightarrow$  PDF of the proton

$f_n(x) \rightarrow$  PDF of the neutron

### • Correction factor $R(x, A)$ :

The function  $R(x, A)$  is a correction factor, 
$$R(x, A) = 1 + 1.19 \ln^{\frac{1}{6}} A [x^3 - 1.5(x_o + x_L)x^3 + 3x_o x_L x] - \left[ \alpha_A \frac{1.08(A^{\frac{1}{3}} - 1)}{\ln(A+1)} \sqrt{x} \right] e^{-x^2/x_o^2}$$

$$x_o = 0.1, x_L = 0.7, \alpha_A = 0.1(A^{\frac{1}{3}} - 1)$$

### ➤ Parton distribution function of the nucleon:

$$xf(x) = A_0 x^{A_1} (1-x)^{A_2}$$

The equation shows the parton distribution function for different types of partons (**d, u, s, and g**) in the nucleon.

$d_v$ :	$A_0 = 1.4473$	$A_1 = 0.6160$	$A_2 = 4.9670$
$u_v$ :	$A_0 = 1.7199$	$A_1 = 0.5526$	$A_2 = 2.9009$
$\bar{u} + \bar{d}$ :	$A_0 = 0.0616$	$A_1 = -0.2990$	$A_2 = 7.7170$
$\bar{d}/\bar{u}$ :	$A_0 = 33657.8$	$A_1 = 4.2767$	$A_2 = 14.8586$
$s = \bar{s}$ :	$A_0 = 0.0123$	$A_1 = -0.2990$	$A_2 = 7.7170$
g:	$A_0 = 30.4571$	$A_1 = 0.5100$	$A_2 = 2.3823$



$$\frac{d\hat{\sigma}}{d\hat{t}} q\bar{q} \rightarrow \gamma^* g = \frac{8\pi\alpha\alpha_s e_f^2}{9\hat{s}^2} \left( \frac{\hat{t}}{\hat{u}} + \frac{\hat{u}}{\hat{t}} + \frac{2M^2\hat{s}}{\hat{t}\hat{u}} \right)$$

$$\frac{d\hat{\sigma}}{d\hat{t}} q\bar{q} \rightarrow \gamma^* \gamma = \frac{2\pi\alpha^2 e_f^2}{3\hat{s}^2} \left( \frac{\hat{t}}{\hat{u}} + \frac{\hat{u}}{\hat{t}} + \frac{2M^2\hat{s}}{\hat{t}\hat{u}} \right)$$

$$\frac{d\hat{\sigma}}{d\hat{t}} qg \rightarrow \gamma^* q = \frac{1\pi\alpha\alpha_s e_f^2}{3\hat{s}^2} \left( -\frac{\hat{u}}{\hat{s}} - \frac{\hat{s}}{\hat{u}} - \frac{2M^2\hat{t}}{\hat{s}\hat{u}} \right)$$

- ❖ First equation shows the process where **a quark and an antiquark produce a virtual photon and a gluon.**
- ❖ Second equation, the process where **a quark and an antiquark produce a virtual photon and a real photon.**
- ❖ Third equation, the process where **a quark and a gluon produce a virtual photon and a quark.**

### Mandelstam variables:

$$s = (p_A + p_B)^2 = p_A^2 + 2p_A \cdot p_B + p_B^2 = 2p_A \cdot p_B,$$

$$t = (p_c - p_A)^2 = -2p_c \cdot p_A,$$

$$u = (p_c - p_B)^2 = -2p_c \cdot p_B,$$

$$\hat{s} = (p'_a + p_b)^2 = p_a'^2 + 2p'_a \cdot p_b + p_b^2 = 2p'_a \cdot p_b = 2z_a x_b \left( \frac{\hat{s}}{2} \right) = x_a z_a x_b s,$$

$$\hat{t} = (p_c - p'_a)^2 = p_c^2 - 2p'_a \cdot p_c + p_a'^2 = -2x_a p_c \cdot p_A = x_a z_a t = -x_a z_a x_2 s,$$

$$\hat{u} = (p_c - p_b)^2 = p_c^2 - 2p_b \cdot p_c + p_b^2 = -x_b p_c \cdot p_B = M^2 + x_b u = -x_b x_1 s,$$

$$\diamond x_1 = -\frac{u}{s} = \frac{1}{2} x_T e^y,$$

$$\diamond x_2 = -\frac{t}{s} = \frac{1}{2} x_T e^{-y},$$

$$\diamond x_T = \frac{2p_T}{\sqrt{s}}$$

$$\diamond \gamma: E^2 = p_T^2 + p_L^2$$

$f_{IP}(x, Q^2) \rightarrow$  Parton distribution function(PDF)

The momentum fraction  $x$

Factorization scale  $Q^2$

Pomeron trajectory  $\alpha_{IP}(\hat{t})$ .

Pomeron flux factor  $A_{IP}$

Momentum transfer

$\alpha$  : fine structure constant

$\alpha_z$  : coupling constant

$\alpha_s$  : strong coupling constant

$e_f$  : electric charge

M : mass of the virtual photon

$\hat{s}, \hat{t}$  and  $\hat{u}$  :Mandelstam variable



哈尔滨工程大学  
HARBIN ENGINEERING UNIVERSITY

---

# 05 Future plan

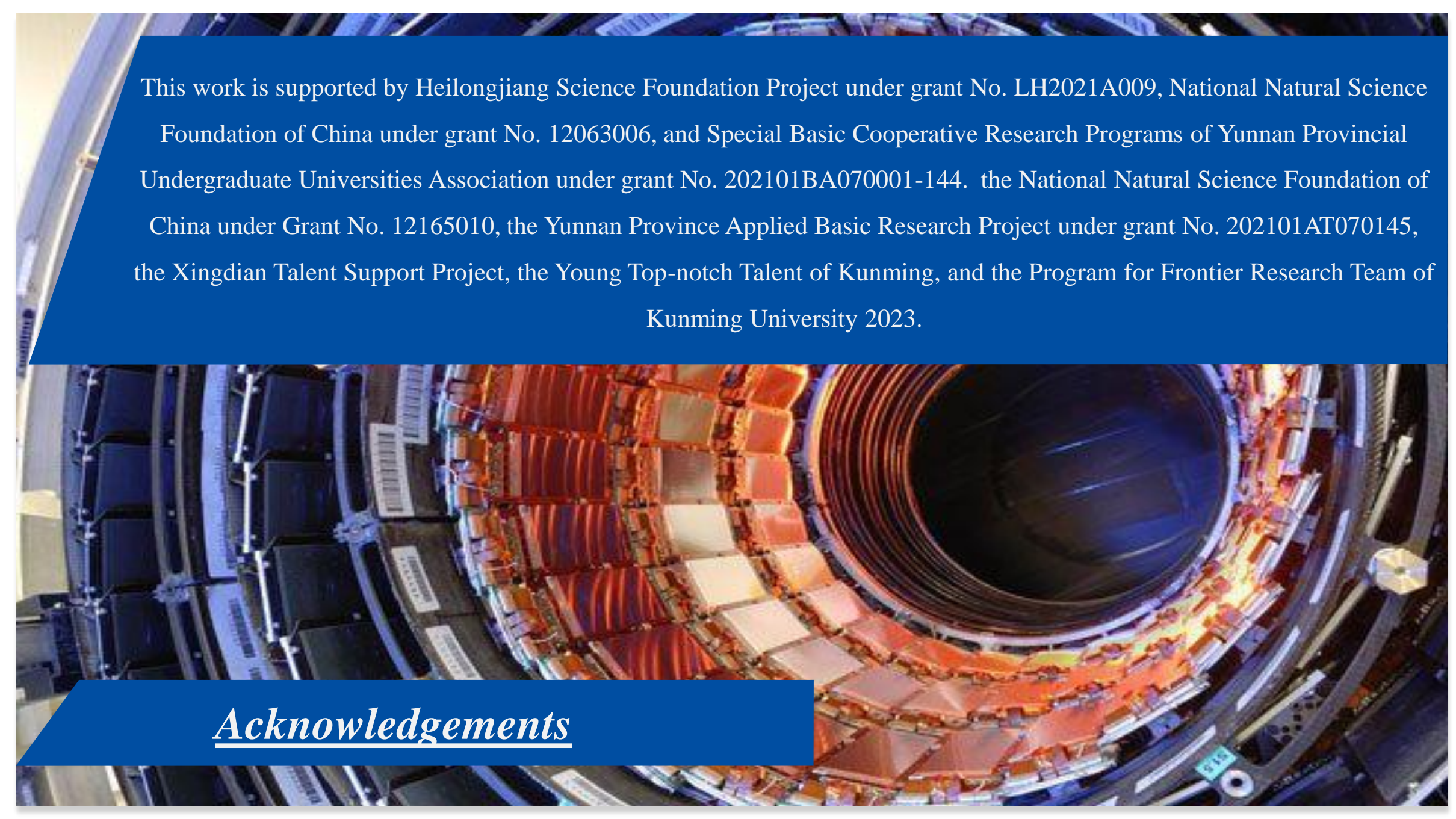




## *Recommendation for further work*

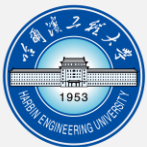
In terms of suggestions for future research, it is crucial to push the boundaries of current methodologies and theoretical models further, to capture the essence of UPCs with even greater precision. Future research should aim at exploring the depths of single and double diffractive production processes at RHIC with defined particles and energies in more granular detail, expanding the horizon of kinematic scenarios examined.





This work is supported by Heilongjiang Science Foundation Project under grant No. LH2021A009, National Natural Science Foundation of China under grant No. 12063006, and Special Basic Cooperative Research Programs of Yunnan Provincial Undergraduate Universities Association under grant No. 202101BA070001-144. the National Natural Science Foundation of China under Grant No. 12165010, the Yunnan Province Applied Basic Research Project under grant No. 202101AT070145, the Xingdian Talent Support Project, the Young Top-notch Talent of Kunming, and the Program for Frontier Research Team of Kunming University 2023.

## *Acknowledgements*



哈爾濱工程大學  
HARBIN ENGINEERING UNIVERSITY

**THANK YOU**

**Rabia Hameed**

